Journal of Sound and Vibration 329 (2010) 4149–4165

Contents lists available at ScienceDirect

Journal of Sound and Vibration

journal homepage: www.elsevier.com/locate/jsvi

Force identification using a statically completed reduced model deriving from tests

M. Corus [a,b,*]

[a] Laboratoire MSSMat, UMR CNRS 8579, École Centrale Paris, Grande Voie des Vignes, 92295 Châtenay Malabry, France
[b] LaMSID, UMR CNRS/EDF 2832, 1 Av. Général de Gaulle, 92141 Clamart cedex, France

ARTICLE INFO

Article history:
Received 10 March 2009
Received in revised form
22 April 2010
Accepted 23 April 2010
Handling Editor: H. Ouyang
Available online 8 May 2010

ABSTRACT

Predicting the operating behaviour of a complex assembly including active components is a challenge, since accurate models of those components are rarely available. For example, the dynamic effects of coupled motor pumps on a nuclear power plant floor are of critical interest, but difficult to predict at the design phase. Indeed, manufacturers do not provide a description of the internal behaviour of the pump, and fluid models can be hard to handle in order to properly define the internal loads. However, the real device and a FE model of the relevant part of the plant are available, and test facilities can be designed.

In this paper, a complete methodology is described to set up a statically complete reduced model of an active component from tests only. This active component is submitted to an internal load. For both the component and the load, no model is available. However, one may need to estimate the behaviour and effects of this component when linked to another structure. First, a statically complete dynamic model of the active component is set up, using a test device reproducing the joints between the active component and the target structure. The use of data expansion techniques on a coarse FE model of the active component, coupled with a tuned FE model of the test device allows the estimation of the residual flexibilities on the interface. Next, a component-dependent equivalent load is identified. Then, test and FE models are combined to compute the forces to apply on the target structure.

A numerical example illustrates the methodology and highlights its practical implementation. Good results are obtained with realistic simulation data. The results also illustrate practical difficulties and limitations.

1. Introduction

Accurate knowledge of structures, including dynamic behaviour and forces, is an important issue from the aspects of repair, diagnosis and maintenance. In a design phase, updated finite element models are widely used to estimate stresses, life expectancy, and in operation behaviour. However, tuned FE models of the structures of interest are not always available. Moreover, due to economic and technical constraints, they cannot be built. For example, EDF (Électricité de France) is in charge of operating and maintaining more than a hundred power plants. It has to analyse, understand and tackle vibration issues on complex structures such as pumps, motors, generators, and many other components, yet not

* Correspondence address: LaMSID, UMR CNRS/EDF 2832, 1 Av. Général de Gaulle, 92141 Clamart cedex, France. Tel.: +33 1 47 65 33 36.
E-mail address: mathieu.corus@ecp.fr

0022-460X/$ - see front matter © 2010 Elsevier Ltd. All rights reserved.
doi:10.1016/j.jsv.2010.04.025

Nomenclature

$[B]_{N\times N_a}$	input shape matrix
$[C]_{N_s\times N}$	output shape matrix
$\{f\}_N$	generalized loads
$[M]$ & $[K]$	mass and stiffness
N	size of the matrix
$\{q\}_N$	model states (i.e. FEM DOF)
$[T]_{N\times N_T}$	reduction basis
$\{u\}_{N_a}$	inputs (i.e. physical loads)
$\{y\}_{N_s}$	outputs (i.e. measurements)
Z	dynamic stiffness

Greek letters

$\{\eta\}_{N_M}$	generalized DOF
$\{\phi_i\}_N$	i th eigen mode
$[\omega]$	natural angular frequencies
$[\Phi]$	normal modes of a FE models
$[\Psi]$	normal modes of reduced models
Ω	active structure (to be identified)
Ω^0	reference device
Ω^1	structure under design or to be qualified with Ω

Superscripts

$\diamond^T$	transpose
$\diamond^0$	relates to Ω^0
$\diamond^1$	relates to Ω^1
$\diamond^{\&0}$	coupled system $\Omega\cup\Omega^0$
$\diamond^{\&1}$	coupled system $\Omega\cup\Omega^1$
$\diamond^+$	pseudo inverse (Moore–Penrose), i.e $\forall A$, $AA^+A=A$ and $A^+AA^+=A^+$, $(A^+A)^T=A^+A$ $(AA^+)^T=AA^+$

Subscripts

$\diamond_a$	actuator (input)
$\diamond_{\mathrm{am}}$	attachment mode
$\diamond_{\mathrm{cm}}$	constraint mode
$\diamond_{\mathrm{cs}}$	correcting shape
$\diamond_C$	complementary (interior) quantity
$\diamond_g$	generalized quantity
$\diamond_{\mathrm{irm}}$	inertia relief mode
$\diamond_I$	interface quantity
$\diamond_L$	local model
$\diamond_r$	reduced quantity
$\diamond_{\mathrm{rb}}$	rigid body
$\diamond_s$	sensor (output)
$\diamond_t$	test quantity (measurements)

having tuned FE models for all the components. To achieve its goals, EDF make several efforts towards measurement, system identification and hybrid modelling [1–3] to set up relevant models of components. Nevertheless, the estimation of the operational behaviour of assemblies, using models deriving from tests, is still an issue. Indeed, in a design phase, or for maintenance or repair purposes, it is critical to estimate the effects of a component under design on an existing assembly, or the effect of an existing structure on a assembly under design. This issue is emphasized when the known structure exhibits internal forces.

EDF has to deal with both sides of the issue. For its new power plants, it needs to design or validate civil engineering structures, where existing pumps, motors or generators will be installed. Since EDF does not manufacture nor design its pumps, motors or generators, these structures are only accessible by tests. On the opposite side, buildings under design cannot be tested, but tuned FE models exist. Reciprocally, it sometimes needs to replace a pump or a motor in an existing installation. In this case, both substructures are only known by tests, but an estimation of the coupled behaviour must be available, for security purposes, before coupling. In both cases, EDF need to compute the coupled operational behaviour of the installation. To achieve this goal, EDF needs tool to set up statically complete models (i.e. allowing coupling in the substructuring techniques sense) of structures, embedding a definition of internal forces, for active components. The case of an active structure (i.e. with internal loads) is addressed in this paper. The needs are summarized in Fig. 1. The main problems to overcome are common interfaces definitions between substructures, the lack of appropriate interface behaviour representation and relevant input forces. In this paper, a complete methodology is introduced to tackle these difficulties.

The first problem is rarely addressed in the literature dealing with test substructuring [4,3], since authors, in general, consider coincident sensors location on the interfaces, when considering experimental substructure coupling [5–8]. To deal with incompatible interfaces, the concept of generalized interface behaviour will be used [9–12]. This technique will be discussed in Section 2. The use of generalized interface behaviour imposes new constraints, relieved by the use of a rough and partial FE model of the structure. This concept of a ''local'' FE model, only used for fields reconstruction purposes, has already been successfully used for structural dynamic modification prediction [13,14,3]. Combined with data expansion techniques, this local FE model creates a kinematic link between measurements and generalized interface behaviour.

The other two issues, the set up of a statically complete model, and of a generalized load, are mainly model-based force identification problems, addressed in Section 3. The set up of a statically complete model strongly depends on the estimation of the residual flexibilities. This problem has been widely studied, and many papers have been published,

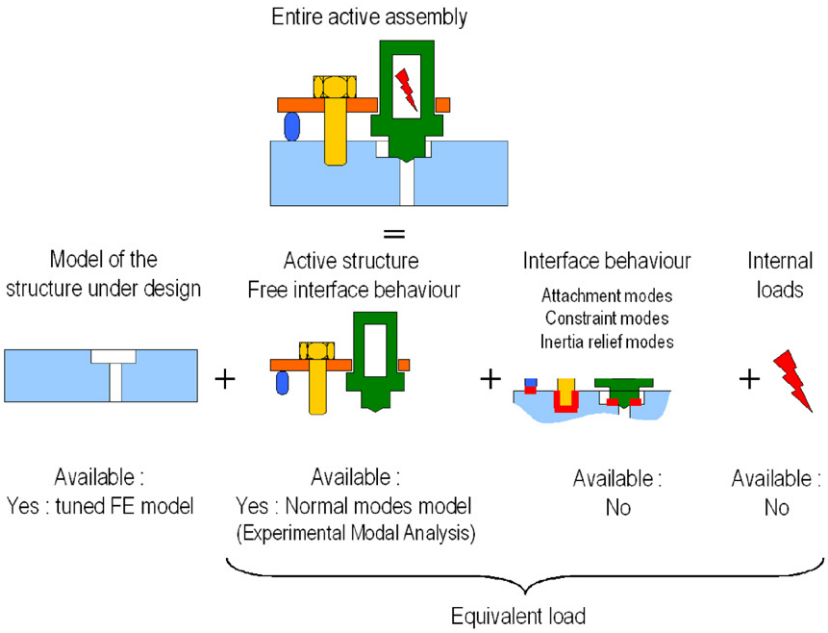

Fig. 1. Details of the needs to build a relevant model of an assembly of structures including an active component.

allowing the estimation of accurate interface behaviour, since measurements are performed on the interface [15–19]. The use of tests performed on coupled system can lead to accurate models of uncoupled components [20,4,21]. The same methodology will be used in this paper. A structure, denoted reference structure, is introduced to estimate the residual flexibilities. This reference structure is assumed to be available to perform both coupled and uncoupled measurements, along with the computation of a tuned FE model.

The last step, for structure with internal forces, is the definition of an equivalent load that takes into account the behaviour of the component. This point is emphasized in Section 4. This equivalent load, which is a generalized model of the component including internal forces, can then be coupled to any other model to estimate in operation behaviour of a complete assembly. The identification of input forces, either internal or external, is an active research field. Many approaches have been proposed in the last few years, addressing this issue. Most of the authors consider an underlying model to estimate loads, either through system identification techniques [22–25], or by solving the inverse problem [26–29]. When considering the inverse problem approach, the system is ill-conditioned, and its inversion thus imposes the use of some regularizing process, such as singular value decomposition, proper order decomposition, modal truncation, spatial filtering or a combination of them [25,26,30,20,31]. In some cases, however, techniques have been developed where the analysis of measurements can directly lead to an estimation of both a reduced model and generalized loads [32–34].

2. Reduced model substructuring

The introduction of a generalized interface behaviour needs the use of a formalism making the difference between the DOF of a model and the quantities of interest. The first section reminds the principles of the model reduction and substructuring using this formalism. The second section presents the definition of the generalized interface behaviour.

2.1. Reduced model substructuring

Component mode synthesis (CMS) is now widely known, and used to reduce the size of FE models for computation purposes [35,36]. It is also a useful tool originally developed to deal with experimentally oriented coupling. The main relationships are reminded using a two components example to introduce the formalism. First, assume that each component has been modelled using FE techniques. Let Z denote the dynamic stiffness of the active structure (resp. Z^0 for the reference device), q (resp. q_0) the displacements. Let C (resp. C^0) be the output and B (resp. B^0) the input shape matrices associated with the interface DOF. B_{ext} (resp. B^0_{ext}) is the input shape matrix associated with external loads. For each

structure, one has the following relations of evolution and observation

$$\begin{cases} [Z]\{q\} = [B]\{u_I\} + [B_{\text{ext}}]\{u_{\text{ext}}\}, \\ \{y_I\} = [C]\{q\}, \end{cases} \tag{1}$$

where y_I (resp. y_I^0) denotes the generalized interface displacements, u_I (resp. u_I^0) the interface loads, and u_{ext} (resp. u_{ext}^0) the external loads. The continuity of the interface displacements, within the subspaces spanned by C and C^0, is written

$$[C \ -C^0]\begin{Bmatrix} q \\ q^0 \end{Bmatrix} = 0, \tag{2}$$

and the nullity of the virtual work, for all the displacement fields q and q^0 verifying (2), gives

$$([C]\{q\})^{\mathrm{T}}([B]\{u_I\}) + ([C^0]\{q^0\})^{\mathrm{T}}([B^0]\{u_I^0\}) = 0. \tag{3}$$

Let $\begin{bmatrix} R \\ R^0 \end{bmatrix}$ denote a basis of the null space of $[C \ -C^0]$. Hence, for each $\begin{Bmatrix} q \\ q^0 \end{Bmatrix}$ verifying Eq. (2), there exist a unique vector $q_r^{\&0}$ verifying

$$\begin{Bmatrix} q \\ q^0 \end{Bmatrix} = \begin{bmatrix} R \\ R^0 \end{bmatrix}\{q_r^{\&0}\}. \tag{4}$$

Each vector $q_r^{\&0}$ then verifies the continuity given by the relation (2).

Substituting (4) and evolution relationships in (3) leads to the coupled problem

$$[R^{\mathrm{T}} \ ZR + (R^0)^{\mathrm{T}} \ Z^0 R^0]\{q_r^{\&0}\} = [R^{\mathrm{T}} \ B_{\text{ext}}]\{u_{\text{ext}}\} + [(R^0)^{\mathrm{T}} \ B_{\text{ext}}^0]\{u_{\text{ext}}^0\}. \tag{5}$$

This formulation is more convenient than the traditional formulation when dealing with reduced models. It is not limited, like the classical formulation, to FE DOF to express coupling conditions. The classical formulation is obtained using Boolean input and output shape matrices. But this approach allows us to define many other interface behaviours, to weaken the coupling conditions, for example, or to deal with incompatible meshes. In the classical formalism, we assume that the DOF of the model can also be partitioned into interface and complementary DOF, so that

$$q = \begin{Bmatrix} q_C \\ q_I \end{Bmatrix} \tag{6}$$

and we then have $[C] = [0_{N_I \times N_C} \ Id_{N_I \times N_I}]$ and $[B] = [C]^{\mathrm{T}}$. In our case, interface DOF are the DOF used to define the generalized interface behaviour.

When dealing with structural dynamics, one may then make the assumption that, for each substructure, there exists a particular basis T (resp. T^0) that can represent the behaviour of the model over a given frequency range. This given basis must represent the distributed forces (and torques, for structural elements) that are transmitted from one substructure to another [37–39,10]. Once a relevant basis is built, generalized displacements fields η give a good estimate of the whole behaviour. They are related to DOF q through the relationship

$$\{q\}_{N\times 1} = [T]_{N\times N_r}\{\eta\}_{N_r\times 1}, \tag{7}$$

where the subscripts N denotes the size of the entire FE model and N_r the size of the reduced subset of generalized DOF, with $N_r \ll N$. This way, the coupled reduced system becomes

$$[(TR_r)^{\mathrm{T}} \ Z(TR_r) + (T^0 R_r^0)^{\mathrm{T}} \ Z^0 (T^0 R_r^0)]\{\eta_r^{\&0}\} = [(TR_r)^{\mathrm{T}} \ B_{\text{ext}}]\{u_{\text{ext}}\} + [(T^0 R_r^0)^{\mathrm{T}} \ B_{\text{ext}}^0]\{u_{\text{ext}}^0\}. \tag{8}$$

2.2. Generalized rigid link between substructures

One of the major advantages of the evolution/observation formulation is the ability to easily take various coupling conditions into account. Indeed, coupling two structures using all the DOF describing the behaviour of the interfaces can lead to unrealistic predictions, inhibiting the motion. This is also useful when different modelizations are used for the two interfaces (3D/beam or 3D/shell), or when interface nodes do not match. The approach which is suggested here is extremely efficient when the complexity of the coupling conditions increases. Generalized coupling condition are easier to take into account [11,40]. One can easily build a generalized motion for each interface, and then directly derive a basis for the kernel of the coupling operator as defined in (4). Such a process is more tedious with the classical approach. Moreover, in most cases, interfaces are described using a large number of DOF, when the overall displacements can be represented using a much lower number of generalized DOF. In the classical Craig and Bampton method, for example, the number of interface DOF is often larger than the number of fixed interface modes used to describe the internal dynamics. Since many papers deal with the reduction of this subspace [10,41,42,9,39], we will only focus on the specific case where we can make the assumption that only the six DOF associated to the rigid body motion of the interfaces are involved. Deriving a more general case is straightforward.

Output shape matrix: Under this assumption, the output shape matrix $C_{I-\mathrm{rb}}$ for each interface can be defined with the relation

$$[C_{I-\mathrm{rb}}] = [\Phi_{I-\mathrm{rb}}]^{\mathrm{T}}[M_{I-\mathrm{rb}}][C_I], \tag{9}$$

where C_I is the input shape matrix allowing the observation of the interface DOF, $\Phi_{I-\mathrm{rb}}$ are the rigid body modes associated to the interface DOF, and orthonormalized with respect to $M_{I-\mathrm{rb}}$, the mass matrix of the interface. This operator will obviously project each interface motion onto the basis of the rigid body modes. However, this definition is not the most convenient, since one must compute a mass matrix related to the interface. This could be done by considering a restraint model of the interface [10], or a statically reduced mass [39]. On the other hand, a set of geometric rigid body modes can easily be computed. Since this operator will be used as an output shape matrix for every interface motion, we do not require any particular scaling. Hence, we could define $C_{I-\mathrm{rb}}$ as a pseudo inverse (denoted $^+$) of these computed rigid body modes. Thus, in the following, we will use

$$[C_{I-\mathrm{rb}}] = [\Phi_{I-\mathrm{rb}}]^{+}[C_I]. \tag{10}$$

Since the number of independent finite element DOF describing the interface is larger than the number of its rigid body modes, the relation (10) leads to a well-conditioned problem. Finite element DOF describing the interface is larger than the number of its rigid body modes, the relation (10) leads to a well-conditioned problem.

Input shape matrix: The definition of $C_{I-\mathrm{rb}}$ allows the projection of any interface motion onto interface rigid body modes. To define the associated input shape matrix $B_{I-\mathrm{rb}}$, it is convenient to consider the dual quantities of the generalized displacements of the interface. Hence, the definition of $B_{I-\mathrm{rb}}$ is straightforward, since we have

$$[B_{I-\mathrm{rb}}] = [C_{I-\mathrm{rb}}]^{\mathrm{T}}. \tag{11}$$

Null subspace basis: For the case of the generalized rigid body motion of the interfaces, let $\left[\begin{smallmatrix} R_{\mathrm{rb}} \\ R^0_{\mathrm{rb}} \end{smallmatrix}\right]$ denote a basis of the null space of $[C_{I-\mathrm{rb}}T \; -C^0_{I-\mathrm{rb}}T^0]$. So, there is a unique vector η^0_{rb} representing the whole behaviour for each state $\left\{\begin{smallmatrix} \eta \\ \eta^0 \end{smallmatrix}\right\}$, and we have

$$\left\{ \begin{array}{c} \eta \\ \eta^0 \end{array} \right\} = \left[\begin{array}{c} R_{\mathrm{rb}} \\ R^0_{\mathrm{rb}} \end{array} \right] \{\eta^0_{\mathrm{rb}}\}. \tag{12}$$

3. Generalized flexibility reconstruction

This section presents the key feature to ensure good equivalent load estimation. In the previous section, reduced model coupling has been presented. Since a tuned FE model of the reference device is available, the set up of a statically complete reduced model of the reference device is straightforward. For the active component, we will use a mixed numerical/experimental approach. The reduction basis adopted for the active component is based on a set of free-interface modes, and needs to be completed with a subset of vectors that represent static deflections of the models submitted to relevant interface loads.

These vectors contain two kinds of data. The first one is the shape of the deformed model under a given load. The second one is the scaling between the amplitude of the resulting displacements and the applied load. In the first section, the construction of generalized correction modes shapes is proposed. This step is supported by a coarse FE model of the active structure. In the second section, the scaling to the proper mechanical behaviour of the active component is presented. To achieve scaling, modal analysis of both the reference structure and the assembly of reference device and active structure are used, in conjunction with data expansion techniques. This step is critical, since the scaling of the correcting shapes directly controls the flexibility of the interface, and then the coupling process.

3.1. Generalized correction shapes

The first step to the set-up of a well-conditioned statically complete representation of the active device is the definition of consistent shapes. These shapes must consistently represent the displacements over the active device for all the interface loads. To build a kinematic relationship between the measurement points and the interface DOF, we propose to build a coarse, local FE model of the instrumented sub domain including reasonable mechanical properties. Other field reconstruction techniques, or analytical results for simple structures, can be used, but the choice of a coarse FE model has many advantages:

- to obtain a quick design and set up of a model depicting the geometry of the active structure, even for complex geometries,
- to ease the construction of smooth displacement fields defined both at measurement points and on the interface,
- to ensure the regularity of the shape functions with respect to the equation of motion.

Moreover, a quick tuning procedure can be set up, so that the first few mode shapes of the local model reasonably match the identified mode shapes of the active component, ensuring the validity of *a priori* computed correction shapes. Let M^L

and K^L denote the mass and stiffness matrix of the local model, and q^L the FE DOF. Since we chose to use generalized links between substructures, the equations defining the main correction shapes need to be adapted.

Generalized constraint modes: Deriving from the construction of the constraint modes [36], the equivalent generalized constraint modes $T_{g-\mathrm{cm}}$ are simply given by considering the generalized interface definition, so that

$$[T_{g-\mathrm{cm}}] = \begin{bmatrix} [Id] \\ -[K_{CC}]^{-1}[K_{Cl}] \end{bmatrix} . [\Phi_{l-\mathrm{rb}}] \tag{13}$$

Generalized residual inertia relief modes: In the case of generalized interface links, the definition of generalized inertia relief modes $T_{g-\mathrm{irm}}$ becomes

$$\begin{cases} [K][T_{g-\mathrm{irm}}] = [M][\Phi_{\mathrm{rb}}], \\ [C_{l-\mathrm{rb}}][T_{g-\mathrm{irm}}] = [0]. \end{cases} \tag{14}$$

Generalized attachment modes: Generalized attachment modes derive from interface loads $B_{l-\mathrm{rb}}$, and are given by

$$[K][T_{g-\mathrm{am}}] = [C_{l-\mathrm{rb}}]^{\mathrm{T}}. \tag{15}$$

When the coupled component exhibits rigid body modes, the relation (15) leads to an ill-conditioned problem. Indeed, for some loading cases, there could be no reaction forces to balance the interface loads. To overcome this issue, Geradin and Rixen [35] have proposed a method with temporary constraints, while Craig [37] proposed to equilibrate interface loads with inertia forces.

Since the range of constraint modes (+ residual inertia relief modes) equals the range of attachment modes (+ rigid body modes), a re-orthogonalization procedure can be used, so that the choice of a particular subset has no importance. It is also the case with generalized correction shapes. In the following, $T_{g-\mathrm{cs}}$ will be built using constraint modes (+ residual inertia relief modes) for convenience.

3.2. Generalized correcting modes tuning

The correction shapes are built thanks to the local FE model of the active device. Since its geometry and overall mechanical properties are relevant with respect to the real structure, computed shapes should give a good estimation of the expected shapes. However, this local FE model is not tuned at all, so these correction shapes cannot be used directly, and beforehand need tuning. To achieve this goal, two different modal analyses will be conducted.

The first one is the modal analysis of the active component alone. A set of experimental modes Φ_t is identified, along with natural frequencies ω_t. This test enables the quick tuning of the local model. The second modal analysis is conducted on the reference device (Ω_0) and the active component (Ω), and will directly be used to tune the scales of the correcting shapes. Let $\Phi_t^{\&0}$ and $\omega_t^{\&0}$ denote the identified mode shapes and natural frequencies of the composite structure $\Omega+\Omega_0$.

3.2.1. Statically complete reduced model of the active component

Once the first modal analysis is performed, and the local FE model is properly set up, we can define a statically complete reduction basis for the active structure. This basis contains the set of n_t free interface experimental modes Φ_t, and the correction shapes $T_{g-\mathrm{cs}}$. Since Φ_t is defined at measurement points, and $T_{g-\mathrm{cs}}$ is defined for the q^L, let C_t^L (resp. C_t^0) denote the output shape matrix allowing the observation of measurements points from local FE DOF (resp. active component FE model). Hence, the vectors of the basis $[\Phi_t\ C_t^L T_{g-\mathrm{cs}}]$ are all defined at measurement points, and are relevant to set up a correct reduced model. However, vectors of Φ_t and $C_t^L T_{g-\mathrm{cs}}$ can be strongly collinear, and then $T_{g-\mathrm{cs}}$ must be filtered to remove any free interface mode contribution from $C_t^L T_{g-\mathrm{cs}}$.

To achieve this goal, vectors of Φ_t are extended over the whole local model. The expansion basis T_t^L used for this purpose is built in two steps. First, attachment modes T_{am}^L are defined, with respect to C_t^L, so that

$$[K^L][T_{\mathrm{am}}^L] = [C_t^L]^{\mathrm{T}}. \tag{16}$$

In the second step, these vectors are sorted with respect to their strain energy, so that

$$[T_t^L] = [T_{\mathrm{am}}^L][\Psi^L], \tag{17}$$

with Ψ_L being the eigenmodes of the local model, reduced on T_{am}^L:

$$[T_{\mathrm{am}}^L]^{\mathrm{T}}(-(\omega_{\mathrm{am}}^L)^2[M^L]+[K^L])[T_{\mathrm{am}}^L]\{\Psi^L\} = 0. \tag{18}$$

A truncated basis will be used in the expansion process. When all the vectors are kept, the result is equivalent to the static expansion result, which is known to well fit the measurements, but also propagates the measurement errors. Using a truncated basis allows control over both the regularity and efficiency of the expansion procedure. This issue has been extensively discussed in [3]. Hence, extended mode shapes Φ_t^L are given by

$$[\Phi_t^L] = [T_t^L][\eta_t^L], \tag{19}$$

η_t^L being the solution of the least square problem defined by

$$[\eta_t^L] = \underset{\eta^L}{\text{ArgMin}}(\|[C_t^L][T_t^L][\eta^L] - [\Phi_t]\|^2). \tag{20}$$

The basis Φ_t^L is then defined on local model's DOF, and it can be used to filter the correction shapes. The complete basis $[\Phi_t^L \ T_{g-\text{cs}}^L]$ is then orthogonalized with respect to M^L and K^L. At this stage, the quick tuning of the local model is important, since the n_t first vectors of the orthonormalized basis must span the same subspace as Φ_t^L, even if the vectors cannot properly be paired, and the eigenfrequencies do not match. It is a critical condition to ensure the proper filtering of $T_{g-\text{cs}}^L$. Let T_r^L denote the filtered basis based on $T_{g-\text{cs}}^L$.

3.2.2. Tuning correction using coupled mode shapes

The new basis $[\Phi_t^L \ T_r^L]$ then contains all the information concerning the shape of the vectors. However, since the local FE model is not a completely tuned FE model of the active component, one cannot ensure the scaling of T_r^L. Indeed, for a tuned FE model, the classical orthogonality relationships should be verified, and thus have

$$\begin{cases} [\Phi_t^L]^{\text{T}}[M^L][\Phi_t^L] = [Id], \\ [\Phi_t^L]^{\text{T}}[K^L][\Phi_t^L] = [\backslash\omega_t\backslash]^2, \end{cases} \tag{21}$$

for the expanded mode shapes. The pseudo pulsation ω_r^L associated to the vectors of T_r^L would define a scale for the correction shapes, and thus we should have

$$\begin{cases} [T_r^L]^{\text{T}}[M^L][T_r^L] = [Id], \\ [T_r^L]^{\text{T}}[K^L][T_r^L] = [\backslash\omega_r^L\backslash]^2. \end{cases} \tag{22}$$

However, this is not the case, and we need to get the proper scales ω_r^L to define the statically complete reduction basis for the active component. The filtering step, along with mass normalization with respect to M^L does ensure

$$\begin{cases} [T_r^L]^{\text{T}}[M^L][\Phi_t^L] = [0], \\ [T_r^L]^{\text{T}}[M^L][T_r^L] = [Id], \\ [T_r^L]^{\text{T}}[K^L][T_r^L] = [\backslash\tilde{\omega}_r^L\backslash]^2. \end{cases} \tag{23}$$

The stiffness contributions $\tilde{\omega}_r^L$ will then be tuned using the modal analysis of the complete structure. Indeed, building a reduced model of the composite structure $\Omega+\Omega^0$ using the reduction basis $[\Phi_t^L \ T_r^L]$ leads to

$$\left(-(\tilde{\omega}_r^{\&0})^2[Id] + \left([R_r]^T \begin{bmatrix} \backslash\omega_t\backslash^2 & 0 \\ 0 & \backslash\tilde{\omega}_r^L\backslash^2 \end{bmatrix}[R_r] + (T^0R_r^0)^{\text{T}}K^0(T^0R_r^0)\right)\right)\{\tilde{\Psi}_r^{\&0}\} = \{0\}, \tag{24}$$

where $\tilde{\Psi}_r^{\&0}$ and $\omega_r^{\&0}$ denote the eigenmodes and eigenfrequencies of the coupled problem.

Note that no assumption is made on T^0. Any method can be used to build this reduced basis. However, due to the purpose of this paper, and the hypotheses made for the coupling conditions (which states that only six DOF related to generalized rigid body motion of the interface are involved), T^0 should include generalized correcting shapes, instead of classical attachment modes or constraint modes. This point will be discussed in Section 4.1.

We will then compare the predicted results with the measurements. Since $\tilde{\Phi}_r^{\&0}$ are defined for generalized DOF, one must first project these generalized shapes onto the test mesh. Let C_t^0 denote the output shape matrix allowing the observation of the reference device FE model DOF. The predicted shapes $\tilde{\Phi}_t^{\&0}$ are then given by

$$\{\tilde{\Phi}_t^{\&0}\} = ([C_t^L][\Phi_t^L \ T_r^L][R_r] + [C_t^0][T^0][R_r^0])\{\tilde{\Psi}_r^{\&0}\} \tag{25}$$

These mode shapes can also be used to compute the eigenmodes of the composite structure defined on both the FE model of the reference device and the coarse FE model of the active component. These modes $\tilde{\Phi}^{\&0}$ are given by

$$\{\tilde{\Phi}^{\&0}\} = ([\Phi_t^L \ T_r^L][R_r] + [T^0][R_r^0])\{\tilde{\Psi}_r^{\&0}\} \tag{26}$$

Let T_g denote the generalized basis $[\Phi_t^L \ T_r^L]$ of the active component.

One then seeks the best stiffness contributions ω_r^L that allows the most accurate prediction of the coupled behaviour $(\tilde{\Phi}_t^{\&0}, \tilde{\omega}_r^{\&0})$. Predicted values are then compared to measurements $(\Phi_t^{\&0}, \omega_t^{\&0})$ to implicitly define an optimization problem. In other words, the objective is to find ω_r^L so that

$$\omega_r^L = \underset{\tilde{\omega}_r^L}{\text{ArgMin}}(\alpha_\omega\|[\backslash\tilde{\omega}_r^{\&0}\backslash] - [\backslash\omega_t^{\&0}\backslash]\|^2 + \alpha_\Phi\|MAC([\tilde{\Phi}_t^{\&0}(\tilde{\omega}_r^L)], [\Phi_t^{\&0}]) - [Id]\|^2). \tag{27}$$

MAC denotes the modal assurance criterion [43] that measures the correlation between the two subsets of shapes, and α_ω and α_Φ are weight coefficients. The first step is conducted with $\alpha_\Phi = 0$ and $\alpha_\omega = 1$, which is the least restrictive function. And, to enhance the quality of the results, α_Φ is increased gradually. Moreover, the choice of the starting values for $\tilde{\omega}_r^L$ is critical. A good choice is to scale the first $\tilde{\omega}_r^L$ with respect to the local model, so that the first iteration is

given by

$$[\backslash\tilde{\omega}_r^L\backslash]^2 = [(T_r^L)^{\mathrm{T}}\ K^L T_r^L]\frac{1}{n_t}\sum_{k=1}^{n_t}\sqrt{\frac{(\omega_t)_k^2}{\{\Phi_t^L\}_k^T[K^L]\{\Phi_t^L\}_k}}. \tag{28}$$

Thus, a reduced model of the active device is available, and statically complete with respect to interface's generalized loads.

3.2.3. Practical aspects linked to the choice of the reference device

The design of the reference structure is an important point ensuring the success of the whole process. Since identification of generalized shapes is performed on the base of coupled behaviour of substructures, the reference device should exhibit the following antagonist properties:

- the coupling interface should be stiff enough, with respect to the active structure. This condition ensures large enough interface loads. A soft interface will lead to great inaccuracies in the scaling process.
- the reference device should not be to stiff, either, to allow measurable displacements, when coupled with the active structure. A stiff reference device will lead to measurements inaccuracies and noise.

The design of a reference structure that will be stiffer than the active structure, but being the same order of magnitude, seems to be a good compromise. With cautious measurements, the behaviour of the reference structure can be accurately identified, while the magnitude of interface loads will reasonably match $\|f\|$.

4. Generalized load identification

Once a complete reduced model of the active device is built, we can set up a generalized load that will have the same effects on the structure under design (Ω_1) as the true loads. Indeed, these loads are impossible to determine without knowing the exact behaviour of the active component. This process is divided into two parts. The first part is a classical force identification process. Having a tuned FE model of the reference device, operating measurements made on the composite structure $\Omega+\Omega_0$ are used to define a set of generalized interface loads f_0 applied to the coupling boundary Σ. In the second part, these generalized interface loads are derived into generalized loads $\tilde{f}$ defined all over the active structure, excluding DOF involved in the interface motion.

4.1. Generalized interface equivalent loads

The first step is to identify generalized equivalent interface loads. Considering relation (8), and replacing the complete state of the composite model $\eta^{\&0}$ with the generalized coordinates associated to each substructure, given by

$$\begin{Bmatrix}\eta_g\\ \eta^0\end{Bmatrix} = \begin{bmatrix}R_r\\ R_r^0\end{bmatrix}\{\eta^{\&0}\}, \tag{29}$$

where $[(R_r)^{\mathrm{T}}\ (R_r^0)^{\mathrm{T}}]^{\mathrm{T}}$ is the basis of the kernel of the observation equation

$$[C_{l-\mathrm{rb}}^0 T^0\ \ -C_{l-\mathrm{rb}}T_g]\begin{Bmatrix}\eta^0\\ \eta_g\end{Bmatrix} = \{0\}, \tag{30}$$

we can express the behaviour of the composite model:

$$[(T_gR_r)^{\mathrm{T}}\ Z(T_g)]\{\eta_g\} + [(T^0R_r^0)^{\mathrm{T}}\ Z^0(T^0)]\{\eta^0\} = [(T_gR_r)^{\mathrm{T}}\ B_{\mathrm{ext}}]\{u_{\mathrm{ext}}\} + [(T^0R_r^0)^{\mathrm{T}}\ B_{\mathrm{ext}}^0]\{u_{\mathrm{ext}}^0\}. \tag{31}$$

Let f denote the true generalized external load, and assume that the reference device is not submitted to an external load. Thus, we have

$$\{f\} = [(T_gR_r)^{\mathrm{T}}\ B_{\mathrm{ext}}]\{u_{\mathrm{ext}}\}. \tag{32}$$

Hence, knowing the overall generalized motion η^0 of the operating reference device, including the interface, directly leads to the expression of f_0.

$$[(T^0R_r^0)^{\mathrm{T}}\ Z^0(T^0)]\{\eta^0\} = \{f_0\} = -[(T_gR_r)^{\mathrm{T}}\ Z(T_g)]\{\eta_g\} + \{f\} \tag{33}$$

Moreover, we made the hypothesis that only the six generalized rigid body motions of the interface are involved in the coupling process. This hypothesis gives us the relation between f_0, the generalized interface loads, and u_{l-rb}^0, the components of the torsor for the interface

$$\{f_0\} = [T^0R_r^0]^{\mathrm{T}}[B_{l-\mathrm{rb}}^0]\{u_{l-rb}^0\} \tag{34}$$

By construction, to ensure static completion, T^0 allows the observation of the rigid body modes of the interface. The relation (34) can be used to project f_0 in order to estimate $u_{l-\mathrm{rb}}^0$, so that

$$\{u_{l-\mathrm{rb}}^0\} = ([T^0R_r^0]^{\mathrm{T}}\ [B_{l-\mathrm{rb}}^0])^+\{f_0\}. \tag{35}$$

Identification of f_0 can be done using classical inversion techniques, but one must be extremely cautious, since results strongly depend on employed techniques. Indeed, since f_0 must be 0 outside the interface, modelling and measurements errors, along with necessary regularization techniques will lead to a generalized load defined all over the reference device. A generalized inversion technique, proposed in [31], will be used to define the generalized interface loads.

In operation measurements are mostly done using one or more reference sensors, other sensors being moved all over the structure under test. To ensure proper phase relations between measurements, cross and auto spectra are built, with respect to the reference sensors. It is seldom possible to come back to stable Fourier transforms of the measurements, and identification processes are conducted using cross and auto spectra information. However, for the sake of clarity, the following presentation will be made assuming that the Fourier transform of the measurements is available. To extend this presentation to cross and auto spectra measurements, one can refer to the work presented in [31], for example.

The main steps of the generalized force identification process are summarized below, assuming that operating measurements $y_t^{\&0}$ are available. $\eta_t^{\&0}$, and then η_t^0 will be computed using the measurements $y_t^{\&0}$.

- Build a proper expansion basis, representing the coupled behaviour of the composite model $\Omega+\Omega_0$.
- Extend operating measurements on the composite model of the reference device and active component.
- Match the restriction of extended data to the reference device with the predefined response of the reference device to generalized interface loads.
- Compute the generalized interface loads using the tuned FE model of the reference device.

The proper reduction basis $\tilde{\Phi}^{\&0}$ for the composite structure is used to perform the modal expansion of the measurements. The reduced model of the active structure is statically complete with respect to the generalized motion of its interface, hence allowing the set up of a relevant coupled model of the composite structure. The reduction basis T^0 is easily built, since a tuned FE model of the reference device is available. The vectors of $\tilde{\Phi}^{\&0}$ are the first eigenmodes computed with the relations (24) and (26), considering the tuned stiffness contribution given by Eq. (27).

We assume here that operating measurements $y_t^{\&0}$ derive from the composite behaviour $\tilde{\Phi}^{\&0}$, so that

$$\{y_t^{\&0}\} = [C_t^{\&0}][\tilde{\Phi}^{\&0}], \tag{36}$$

where $C_t^{\&0}$ is the output shape matrix representing the observation of the measurements from the DOF of the complete composite FE model.

Hence, operating measurements are extended using a least mean square minimization. For each frequency of interest, the motion defined on all the FE DOF (both reference device and active component) $q_t^{\&0}$ is given by

$$\{q_t^{\&0}\} = [\tilde{\Phi}^{\&0}]\{\eta_t^{\&0}\}, \tag{37}$$

where generalized operating DOF $\eta_t^{\&0}$ are given by

$$\{\eta_t^{\&0}\} = \underset{\eta^{\&0}}{\mathrm{ArgMin}} |[C_t^{\&0}\tilde{\Phi}^{\&0}]\{\eta^{\&0}\} - \{y_t^{\&0}\}|^2. \tag{38}$$

The number of sensors must then be at least as large as the number of vectors of $\tilde{\Phi}^{\&0}$ to ensure that $[C_t^{\&0}\tilde{\Phi}^{\&0}]$ is full rank. The solution is then given by

$$\{\eta_t^{\&0}\} = ([C_t^{\&0}\tilde{\Phi}^{\&0}])^+\{y_t^{\&0}\}. \tag{39}$$

Direct solution for generalized load definition: Once the motion is defined over the entire composite model, the computation of f_0 is straightforward. The generalized interface loads f_0 are simply given by

$$\{f_0\} = [T^0 R_r^0]^{\mathrm{T}}[Z^0]([C_0^{\&0}]\{q_t^{\&0}\}), \tag{40}$$

where $C_0^{\&0}$ can extract the DOF of the reference device model from the complete composite model.

However, this subspace can be too large to ensure a proper expansion result. Hence, one must choose a reduced subspace to ensure the regularity of the solution. This can be efficiently done by sorting the vectors of T^0 with respect to strain energy, and by considering only the lowest order shapes. An alternate technique, based on the same principles as the generalized flexibility reconstruction problem, can be used.

Preferred solution for generalized load determination: We are interested in generalized interface load estimation within a given frequency band. Thus, we assume that the restriction of $q^{\&0}$ to the reference device alone can be represented on a subspace including both free interface modes Φ^0 of the reference device, and its static responses $T^0_{g-\mathrm{am}}$ to generalized interface loads. An input shape matrix $B^0_{I-\mathrm{rb}}$ is built considering the technique proposed in Section 2.2. Hence, considering the rigid body motion of the interface DOF, the static responses $T^0_{g-\mathrm{am}}$ are built. As for the construction of T^L_{g-cs}, many options are available. The complete basis $[\Phi^0\ T^0_{g-\mathrm{am}}]$ is then orthonormalized with respect to the tuned FE model of the reference device. Let T_g^0 denote this reduction basis.

The next step consists in determining the contribution of the vectors of T_g^0 in $q^{\&0}$. Since the reference device is only submitted to the reaction of the active components, the restriction of $\tilde{\Phi}^{\&0}$ to the reference device model's DOF and T_g^0

should span the same subspace. If $T^0=T_g^0$, the same basis used to build the composite model, then this assertion is obvious. Other reduction bases can be used in Eq. (24) to build the composite model, but since they all need to be statically complete with respect to the interface, one ensures that T_g^0 is included within the restriction of $\tilde{\Phi}^{\&0}$. Hence, the set up of T_g^0 and so of $\tilde{\Phi}^{\&0}$ are of critical importance.

Hence, one can easily determine the contribution η_t^0 of the vectors of T_g^0 within the restrictions of $\tilde{\Phi}^{\&0}$. Let $C_0^{\&0}$ denote the output shape matrix allowing the observation of the reference device FE model from the composite structure model. η_t^0 is given by

$$\{\eta_t^0\}=[T_0^{\&0}]\{\eta_t^{\&0}\}, \tag{41}$$

where $T_0^{\&0}$ is the linear mapping between both subspaces,

$$[T_0^{\&0}]=\underset{T}{\mathrm{ArgMin}}|[T_g^0][T]-[C_0^{\&0}][\tilde{\Phi}^{\&0}]|^2. \tag{42}$$

In this case, since the number of DOF of the reference device FE model is larger than the number of vectors of T_g^0, the inverse problem is well conditioned, and $T_0^{\&0}$ is full rank. This problem can be solved using the pseudo inverse of T_g^0

$$[T_0^{\&0}]=[T_g^0]^+([C_0^{\&0}][\tilde{\Phi}^{\&0}]). \tag{43}$$

As operating motion is defined for the reference device, the generalized interface loads f_0 are directly given by

$$\{f_0\}=[T_g^0R_r^0]^{\mathrm{T}}[Z^0][T_g^0]\{\eta_t^0\}. \tag{44}$$

Note: Operators R_r^0 and R_r cannot be used to compute η_t^0 from $\eta_t^{\&0}$, since $\eta_t^{\&0}$ are the generalized coordinates associated to the basis $\tilde{\Phi}^{\&0}$, when η_t^0 is related to T_g^0 (or T^0). We could have used the reduced modes $\tilde{\Psi}_r^{\&0}$, defined in the relation (24), to switch the bases, instead of relation (43). One can show that both results are the same.

In the following, we will use T_g^0 instead of T^0.

4.2. Equivalent generalized load

Generalized interface loads being defined on the reference device, the last step is the determination of an equivalent generalized load $\tilde{f}$ on the active device. We seek a load that would have on Ω_0 exactly the same effects as the true load f. Assuming such $\tilde{f}$ exists, it would then verify

$$[(T_g^0R_r^0)^{\mathrm{T}}\ Z^0(T_g^0)]\{\eta_t^0\}+[(T_gR_r)^{\mathrm{T}}\ Z(T_g)]\{\tilde{\eta}\}=\{\tilde{f}\}, \tag{45}$$

Displacements $q_t^0=[T_g^0R_r^0]\eta_t^0$ on Ω_0 are the same, but generalized displacements $\tilde{\eta}$ on Ω may be different, since only generalized interface motion is constrained.

Substituting Eqs. (33) and (45) gives the expression of the generalized load $\tilde{f}$

$$[(T_gR_r)^{\mathrm{T}}\ Z(T_g)]\{\tilde{\eta}\}=\{\tilde{f}\}-\{f_0\}, \tag{46}$$

Given a particular generalized solution $\tilde{\eta}$, one can then estimate the related generalized load $\tilde{f}$. In Section 4.1, we have built a generalized displacement $\eta_t^{\&0}$, based on Eqs. (36), (37) and (38). This solution can then readily be used to compute a generalized solution $\tilde{\eta}$ for the active structure in the same way as η_t^0 was computed from $\eta^{\&0}$. Hence, we can have

$$\{\tilde{\eta}\}=[\tilde{T}_0]\{\eta_t^{\&0}\}, \tag{47}$$

where $\tilde{T}_0$ is the operator allowing the transition between the subspaces, hence

$$[\tilde{T}_0]=\underset{T}{\mathrm{ArgMin}}|[T_g][T]-[C^{\&0}][\tilde{\Phi}^{\&0}]|^2, \tag{48}$$

where $C^{\&0}$ can extract the DOF of the active component model from the complete composite model. The number of DOF of the coarse FE model of the active component is larger than the number of vectors of T_g, the inverse problem is well conditioned, and $\tilde{T}_0$ is full rank.

Combining the various relations, and replacing in (46), leads to the expression of $\tilde{f}$ as a function of the models, the reduced bases and the measurements only:

$$\{\tilde{f}\}=([(T_g^0R_r^0)^{\mathrm{T}}\ Z^0(T_g^0)][T_g^0]^+[C_0^{\&0}])+[(T_gR_r)^{\mathrm{T}}\ Z(T_g)]([T_g]^+[C^{\&0}])[\tilde{\Phi}^{\&0}]([C_t^{\&0}\tilde{\Phi}^{\&0}])^+\{y_t^{\&0}\} \tag{49}$$

Eq. (49) is then applied for each frequency step to compute the generalized load $\tilde{f}$. This solution is completely driven by the measurements and the reduced bases T_g^0 and T_g, since $\tilde{\Phi}^{\&0}$ is also based on these bases. If $[T_g^{\mathrm{T}}ZT_g]$ is a good reduced FE model of the active component, and if T_g^0 and T_g are well suited to represent the dynamics within the relevant frequency range, $\tilde{f}$ will tend towards f when the number of sensors increases, hence when $y_t^{\&0}$ tends to $q_t^{\&0}$. It also appears that the choice of the reduced basis T_g is critical. Indeed, performing a good static completion, as described in Section 3, will ensure the construction of relevant coupled modes $\tilde{\Phi}^{\&0}$, and then the quality of the generalized load $\tilde{f}$.

By construction, the use of $\Psi_r^{\&0}$ allows us to switch between bases, so that $\tilde{f}$ is also given by

$$\{\tilde{f}\} = [(T_g^0 R_r^0)^{\mathrm{T}} \; Z^0 (T_g^0 R_r^0) + (T_g R_r)^{\mathrm{T}} \; Z (T_g R_r)][\Psi_r^{\&0}]([C_t^{\&0} \tilde{\Phi}^{\&0}])^+ \{y_t^{\&0}\}. \tag{50}$$

$\tilde{f}$ is a generalized load defined for the reduction bases T_g and T_g^0. In order to use this equivalent load as an input for another composite model, including the active component, one may define an equivalent input shape matrix $\tilde{B}$. It can simply be done by using relation (32). In our case, the projection basis for $\tilde{f}$ is $\Phi^{\&0}$, hence $\tilde{B}$ can directly be computed using

$$[\tilde{B}] = ([C^{\&0}[\tilde{\Phi}^{\&0}]])^+. \tag{51}$$

5. Numerical example

In this section, a numerical experiment is built to validate the methodology previously defined, and summarize the different steps. Simple FE models representing the reference device and the active component are given. An internal load f is defined. Experimental modal analysis and operating measurements for the reference device, the active component and the composite structure are simulated. The main steps of the whole process are reproduced in the example.

For the purpose of the demonstration, a third structure is introduced. This structure, denoted Ω_1, simulates the structure under design, and is coupled with the active component. This composite model will be submitted both to internal load f, and to the identified equivalent load $\tilde{f}$.

5.1. FE models and hypotheses

This example is conducted in the same way as in a real life situation. FE models of a reference device, an active component, and the structure under design are built. The assemblies representing the composite structures $\Omega+\Omega_0$ and $\Omega+\Omega_1$ is presented in Fig. 2.

These models could represent a pump, the reference test bed designed by the pump manufacturer, and the part of the floor where the pump should be located. The reference test bed and the floor are clamped on their lowest sides, and the pump is bolted to the reference device or the floor. A distributed load is defined inside the pump, whose torsor, taken at the interface, have no zero value. This aims to simulate the complex behaviour of both fluids and rotating parts. These models have been designed to meet the typical dynamic properties of the structures of interest at EDF. The study will be conducted on the [0–100 Hz] frequency range. The first and tenth frequencies of the three structures and two assemblies are summarized in the Table 1. According to the Section 3.2.3, the reference device should be stiffer than the active component. However, the choice of building a realistic example lead us to a slightly softer structure.

To simulate the test results, experimental meshes are defined for the reference device and the active component. A total amount of 161 sensors are defined, 60 for the active component, and 101 for the reference device. For the active component, the choice of measuring the three directions at each point has been made. It is supposed to be an unknown structure, so some efforts should be made for the measurements. Concerning the reference device, its geometry and behaviour should be simple, but the need of a fine tuned FE model imposes some fine measurements. However, its behaviour can be fairly well estimated using a coarse FE model, so we choose to have numerous sensor locations and few measurements directions. This configuration aims to represent a realistic test case that could be used to experimentally validate the methodology.

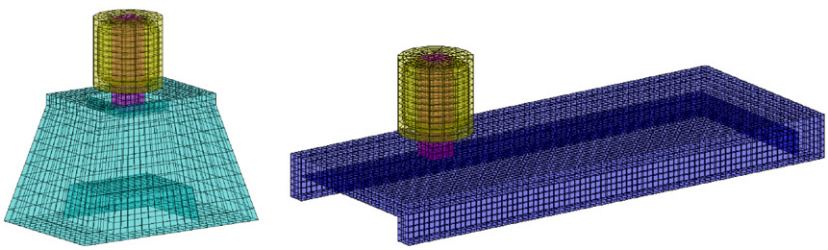

Fig. 2. FE model of the reference device + active component assembly (left) and of the structure under design + active component assembly (right).

Table 1
Frequencies of the first and tenth eigenmodes for each structure/substructure assembly.

Mode #	Ω_0 (Hz) (reference)	Ω (Hz) (active)	$\Omega_0+\Omega$ (Hz)	Ω_1 (Hz) (under design)	$\Omega_1+\Omega$ (Hz)
1	47.7	99.3	15.7	27.3	11.0
10	163.2	160.0	96.7	69.3	53.2

Reference results have been computed using complete models of assemblies, assuming 1 percent of modal damping. Experimental modal analyses should be conducted within an extended frequency range, to limit the modal truncation effects, and every mode within this frequency range is supposed to be properly identified. Modes up to 150 Hz are retained for this analysis. This assumption is relevant, considering that this includes the first eight modes for both the reference device and the active component.

5.2. Reduced model using generalized rigid body interface motion

The coupling area is limited to 16 nodes, since only the bottom face of the active device will be coupled to the other structures. For the complete FE model assemblies, the interfaces are assumed to be perfectly glued, and every FE DOF will be involved in the coupling. For the reduced models, the coupling conditions will be built based on generalized rigid body interface motion hypothesis, as described in Section 2.2, since the coupling area is small, and stiff with respect to the complete assembly.

To validate this approach, a comparison between the results obtained with the complete model, and the assembly of the reduced model is conducted. The results are very good within the frequency range [0–100 Hz]. We have no more than 2 percent of error on the frequency prediction, with MAC values no less than 97 percent for the first 10 modes in each configuration, hence validating this hypothesis. All the frequencies are slightly under estimated. This phenomenon is due to the reduction basis used to describe the interface behaviour. This phenomenon should be carefully examined, since it is the key of the success of this coupling procedure. If the coupling areas were not stiff enough, with respect to the complete structure, assuming a generalized rigid body motion for the interface would lead to inaccurate results. In our case, this assumption is fairly well verified, and the assumption of a generalized rigid body interface motion leads to good coupled results.

5.3. Reconstruction of the correction shapes flexibilities

This study is conducted using eight modes for the reference device and 14 (including the six rigid body modes) for the active component. Correcting shapes are built considering generalized rigid body motion of the coupling interface, using the generalized inertia relief mode shapes. These shapes are orthonormalized with respect to the eight flexible modes already available and the six computed rigid body modes. Fig. 3 presents the starting point, and the result of the optimization procedure. The reference model is the complete FE model of the assembly.

Since the complete basis is orthonormalized, the starting point for the generalized flexibilities should be higher than the last flexible frequency f_{max} of the active component. The six starting points for the optimization process are chosen according the criterion given in Section 3.2.2 to verify this assumption. They are slightly adjusted to ensure a good convergence of the minimization process. The minimization focuses on the first 10 modes, including criteria on both MAC and frequencies.

The optimization process is very efficient. The model with the optimized stiffness contributions provides better results than the true reduced model, presented in Section 5.2. For the first 10 modes, all the MAC values are 1, and the error in the frequency prediction is less than 0.1 percent. The correction shapes used in this process are the true shapes, since the local FE model used is also the true FE model of the active component. Using different models would induce different shapes, in such a way that the results are not likely to be as much satisfactory. However, the underlying principles are validated, and a fair estimation of the residual flexibilities can be obtained, thanks to the optimization. The robustness of such process with respect to the local FE model has been extensively studied in [3].

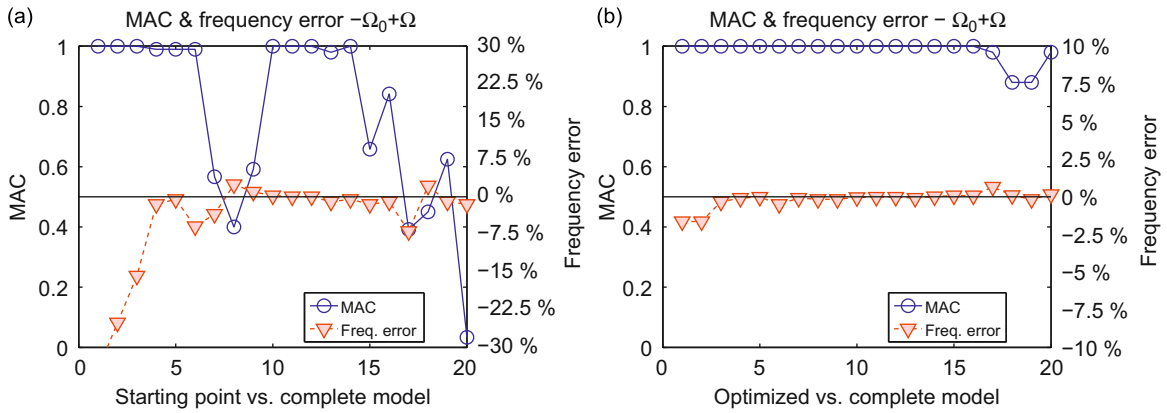

Fig. 3. MAC and frequency relative errors for the starting point of the optimization (a) and the optimal flexibilities (b).

It must be noted, however, that the success of the process is strongly linked to both measurements and coupled models. All the correction shapes should have a significant effect on the coupled modes, and they all need to be involved in the identified modes. Indeed, if a particular correction shape has no effect on the coupled behaviour, or if it has a critical influence on a particular coupled mode that is not identified, the associated stiffness contribution will not be efficiently estimated. This can also lead to conditioning issues for the optimization procedure. Hence, if a particular shape has no significant role in the coupling process, it should better be removed from the correction shapes subset.

5.4. Reconstruction of the interface load f_0

The next step is the estimation of the interface load f_0 transmitted by the active device to the reference structure. Operating measurements have been simulated, and measurements defined at sensors are expanded on the calculated mode shapes of the reduced model $\tilde{\Phi}^{\&0}$ of the composite structure $\Omega+\Omega_0$. As stated in the theoretical part of this paper, the choice of the expansion basis governs the prediction results. A guideline for the selection of relevant vectors in the expansion basis is proposed in this section, and results illustrating the influence of these choices are proposed.

Let $N_{m\ 0}$ (resp. N_m) denote the number of modes identified for the reference device (resp. for the active component). Assuming that six generalized correcting shapes are added to each reduced model, a total of $N_m+N_{m\ 0}+6$ modes $\tilde{\Phi}^{\&0}$ have been computed. If we have more sensors than computed modes, the expansion process is well conditioned. If more modes than sensors are computed, the size of the expansion should be reduced. This can be performed either by keeping only the first computed modes of $\tilde{\Phi}^{\&0}$, or by choosing less modes for each reduced model of the components. Several choices are discussed below.

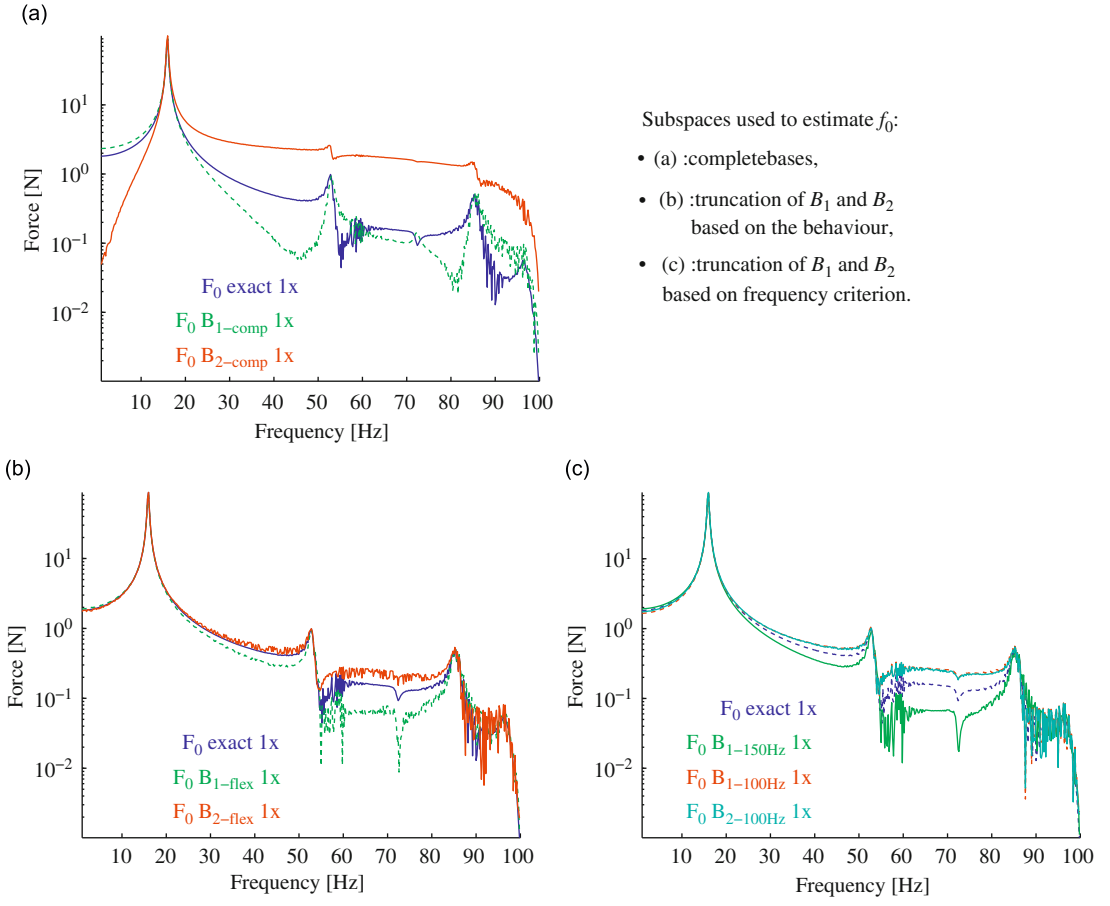

Fig. 4. Estimation of f_0 in the $\vec{x}$ direction with complete and truncated bases deriving from B_1 and B_2—comparison with reference results (dark blue) (For interpretation of the references to colour in this figure legend, the reader is referred to the web version of this article.).

To illustrate the effects of the choices in the expansion basis and in the truncation, two expansion bases B_1 and B_2 are computed. They both correspond to all the coupled modes of the composite reduced models, built with different parameters. $[B_1]$ is computed using

- eight modes (up to 150 Hz) for the reference device, and six generalized flexibility correcting shapes,
- 14 modes (up to 150 Hz) for the active component, including the six rigid body modes, and the six generalized flexibility correcting shapes,

and $[B_2]$ is computed using

- five modes (up to 110 Hz) for the reference device, and six generalized flexibility correcting shapes.
- nine modes (up to 110 Hz) for the active component, including the six rigid body modes, and the six generalized flexibility correcting shapes.

There are 28 vectors in B_1, and 20 in B_2. It should be noted that when changing the number N_m of free modes in the active component reduced model, the optimization problem should be solved to compute the optimal stiffness contributions associated with this particular basis.

Some other bases are derived from B_1 and B_2:

- Truncation based on the behaviour: $[B_{1-\text{flex}}]$ and $[B_{2-\text{flex}}]$, where all the relevant predicted mode shapes are kept, hence all but the last six. Indeed, for two components, we have 12 correction shapes, six for each component. By construction, for each correction shape, we have a relevant behaviour for a given substructure, while imposing a null behaviour on the other. Ensuring the continuity on the interface using these 12 shapes imposes six constraints, so only six shapes are well defined, corresponding to static deflection of the coupled model for generalized rigid body motion of the interface. The other six shapes should be null shapes, leading to six spurious shapes in the coupled model.

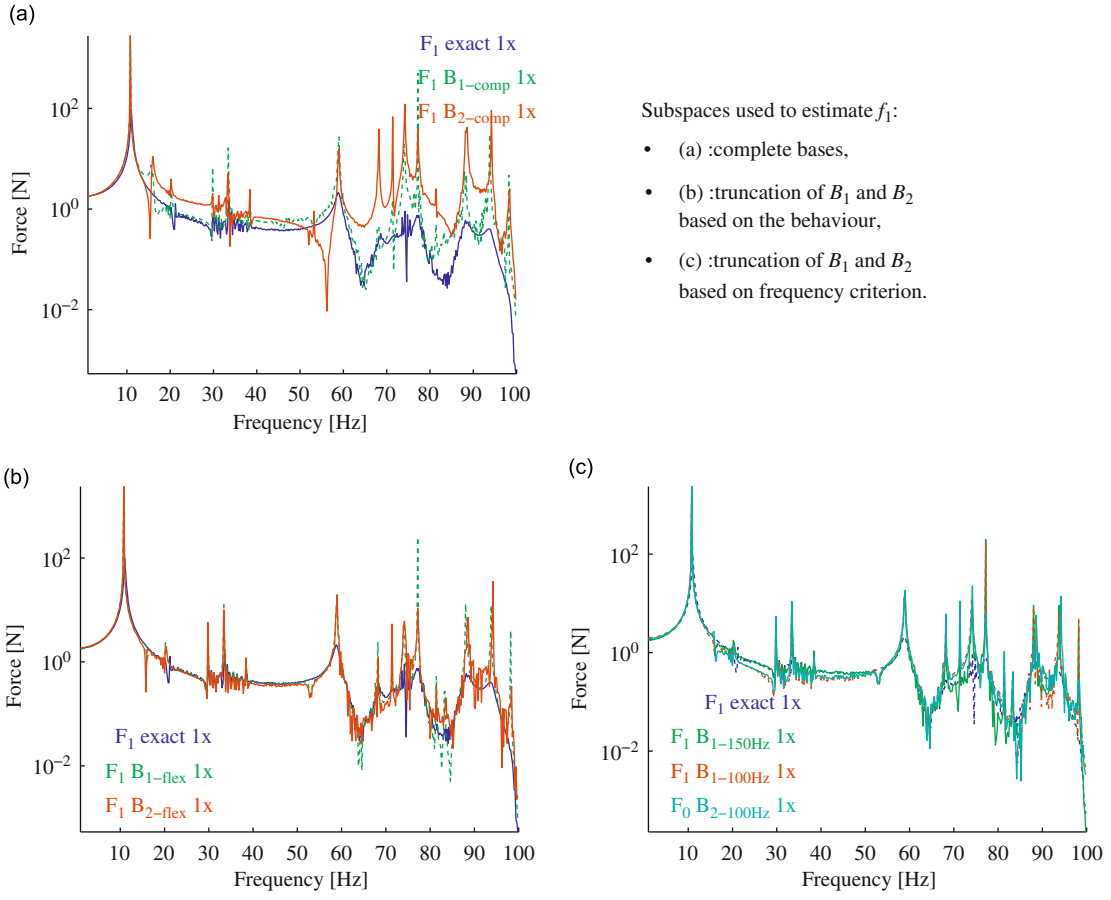

Fig. 5. Estimation of f_1 in the $\vec{x}$ direction with complete and truncated bases deriving from B_1 and B_2—comparison with reference results (dark blue) (For interpretation of the references to colour in this figure legend, the reader is referred to the web version of this article.).

- Truncation based on the frequency: $[B_{1-150\,\mathrm{Hz}}]$, $[B_{1-100\,\mathrm{Hz}}]$ and $[B_{2-100\,\mathrm{Hz}}]$, where only the coupled modes associated with frequencies less than 150 and 100 Hz are kept. There are 20 vectors in $[B_{1-150\,\mathrm{Hz}}]$, and 12 in $[B_{1-100\,\mathrm{Hz}}]$ and $[B_{2-100\,\mathrm{Hz}}]$. It is noted that $[B_{1-100\,\mathrm{Hz}}]$ and $[B_{2-100\,\mathrm{Hz}}]$ should be equal.

In this example, the sizes of both bases are smaller than the number of sensors. Nevertheless, we will investigate the effects of the truncation on the reconstruction process. It is not *a priori* clear, indeed, what option should be preferred. On one hand, reducing the size of the expansion basis itself will also limit the noise propagation in the reconstruction process, but will limit the observation of the highest order modes. On the other hand, accounting for the highest order modeshapes should increase the accuracy of the estimation, but will affect the conditioning of the inverse problem. The right truncation is the best compromise between these two effects. The competition between these effects is illustrated in Fig. 4. The reference solution, denoted "exact", is computed with the full FE models of the composite assembly, and of the reference device to derive f_0.

When the complete bases are used, the estimation of the load in the $\vec{x}$ direction is not satisfactory. The low frequency estimation computed with B_1 is good, but higher frequencies components are not well estimated outside the main resonance frequencies. The results computed with B_2 are not accurate at all, the quasi-static contributions of some higher order modes are not well taken into account. All these phenomena derive from the presence of the last six spurious modes in both B_1 and B_2.

Reducing the size of the basis significantly increases the quality of the estimation. Eliminating the spurious shapes leads to fairly accurate results. The basis $(B_{2-\mathrm{flex}})$ leads to the closest estimation, but results are noisy, since the last coupled modeshapes are not well estimated. Using frequency based truncation slightly deteriorate the estimation, but noise is quite completely eliminated when load levels are significant. It can be noted that the bases $B_{1-100\,\mathrm{Hz}}$ and $B_{2-100\,\mathrm{Hz}}$ lead to the same results, as expected. It should also be noted that the size of the expansion basis directly influences the results. The load is overestimated when few vectors are used, and underestimated when a large number of vector is used to perform the data expansion. However, the load peaks are well estimated in all cases, when considering truncated bases. The good choice is then to build an expansion basis relevant with the frequency range of interest for the load identification. Larger bases could lead to model inconsistencies.

5.5. Reconstruction of the equivalent load $\tilde{f}$ and estimation of f_1

At this stage, we can estimate the generalized equivalent load $\tilde{f}$ to be applied to the active device, coupled with any structure. In order to validate the accuracy of the reconstruction, the estimated load $\tilde{f}$ is applied to the composite model $\Omega+\Omega_1$, and the equivalent interface load f_1 between the active component and the structure being designed is computed. The quality of the reconstruction of f_1 will then be a fair estimator for the reconstruction of $\tilde{f}$, since it measures the load that will be transmitted to the structure under design. The estimations of f_1 have been computed with the variants of bases B_1 and B_2 defined in Section 5.4.

Fig. 5 presents the results computed using the various expansion bases. We note that all bases lead to estimations that exhibit spurious peaks. These peaks are located at the resonant frequencies of the composite model $\Omega_0+\Omega$. They derive from the construction of generalized load $\tilde{f}$. The estimation of the generalized load $\tilde{f}$ is strongly distorted near the resonance frequencies of the system used to perform the identification. These errors derive from the estimation of the complete behaviour from test results, caused by the expansion process. Using data from a larger number of sensors could significantly lower these errors in the generalized loads. Moreover, some data treatment can also be performed to lower these errors, since their locations are known. If one can assume some regularity for the true load spectra, this can be used to smooth the results. Assuming a generalized rigid link between the structures also limits error propagation. Reducing the size of the subspace describing the interface loads introduces some regularization in the process, acting as a spatial filter.

However, theses results are good. Estimations obtained using the full bases are not accurate, but reducing the size of the basis significantly increases the quality of the results. In this case, both truncation approaches lead to very good results. These results confirm the good behaviour of the proposed methodology to estimate the main loads. Effects in all the directions are well estimated, assuming that the expansion basis can introduce some important data linked to the higher modes, while keeping a reasonably low conditioning number.

6. Conclusion

In this paper, a complete methodology is described to set up a statically complete reduced model of an active component from tests only. This active component is submitted to an internal load. For both the component and the load, no model is available. However, one may need to estimate the behaviour and effects of this component when linked to another structure.

First, static completion is achieved using results from tests made on the active component with different boundary conditions. In each case, the boundary conditions need to be well known to derive a relevant model. Hence, free-free boundary conditions are used, as well as coupling with a simple and easy to build model of the reference device. Hypotheses about the interface behaviour are made to introduce a generalized link between the structures. The use of data

expansion techniques on a coarse FE model of the active component, coupled with a tuned FE model of the reference device allows the estimation of residual flexibilities for the interface.

The second major step is the set up of a generalized load defined on the active component inducing on any other structure the same effects as the "true" internal loads, assumed to be unknown and unreachable. The inverse problem based on operating measurements and tuned FE model of the reference test bed is solved, to determine an equivalent loading on the coupling interface. Combined with the statically complete model of the active structure, a generalized load is computed.

A realistic numerical test case is set up, representing a motor pump on a nuclear plant floor. The motor pump is the active component, only known by the manufacturer, and submitted to the internal loads. The complete method is implemented. A reference device is introduced, and test results have been simulated. This reference device should realise the compromise between the measurements and the inverse problem. To ensure good measurements, it should not be too stiff, hence allowing good interface displacements estimations. But it should be reasonably stiff to limit conditioning issues with the inverse problem. The efficiency of the residual flexibility estimation is presented, along with the relevance of the generalized link hypothesis. Interface loads deriving from the internal loads are found, and compared to reference numerical results. A generalized load coupling the interface load and the complete reduced model is computed, and compared to the reference load. In each case, very good results are obtained. As the method relies on data expansion, some keys are given to better estimate the solution using *a priori* considerations. Some limitations linked to the test set up are also discussed.

The next step is to propose an experimental validation of the estimation of a statically complete reduced model. Some academical devices are tested, and results for various boundary conditions will be presented. Once done, an internal load will be simulated using a shaker, and the complete inverse problem will be solved.

Acknowledgements

This research was funded by the EDF (Électricité de France) Research and Development division. The author would like to thank Emile Luzzato, Patrick Massin and Laurent Billet for their supports.

References

[1] B. Salhi, J. Lardies, M. Berthillier, Identification of modal parameters and aeroelastic coefficients in bladed disk assemblies, *Mechanical Systems and Signal Processing* 23 (2009) 1894–1908.
[2] A. Batou, C. Soize, Experimental identification of turbulent fluid forces applied to fuel assemblies using an uncertain model and fretting-wear estimation, *Mechanical Systems and Signal Processing* 23 (2009) 2141–2153.
[3] M. Corus, E. Balmes, O. Nicolas, Using model reduction and data expansion techniques to improve sdm, *Mechanical Systems and Signal Processing* 20 (2006) 1067–1089.
[4] C. Koh, K. Shankar, System identification of substructures without interface measurements, *ASCE Journal of Engineering Mechanics* 129 (7) (2003) 769–776.
[5] D.J. Ewins, *Modal Testing: Theory, Practice and Application*, second ed., Research Studies Press, Letchworth, Hertfordshire, UK, 2000.
[6] L. Jezequel, H.D. Seito, Component modal synthesis methods based on hybrid models part 1: theory of hybrid models and modal truncation methods, *Journal of Applied Mechanics* (1994) 100–108.
[7] W. Liu, Structural Dynamic Analysis and Testing of Coupled Structures, PhD Thesis, Imperial College of Science, Technology and Medicine, University of London, 2000.
[8] G.W. Skingle, Structural Dynamic Modification Using Experimental Data, PhD Thesis, Imperial College of Science, Technology and Medicine, University of London, 1989.
[9] R.R. Craig, C.J. Chang, Substructure coupling for dynamic analysis and testing, NASA CR-2781, 1977.
[10] F. Bourquin, F. D'Hennezel, Numerical study of an intrinsic component mode synthesis method, *Computer Methods in Applied Mechanics and Engineering* 97 (1992) 49–76.
[11] E. Balmes, Use of generalized interface degrees of freedom in component mode synthesis, *International Modal Analysis Conference* (1996) 204–210.
[12] H. Ben Dhia, E. Balmes, Mesure de compatibilité et application aux problèmes de sous-structuration, *Colloque National en Calcul des Structures*, Giens, 2003.
[13] P. Avitabile, J. O'Callahan, C.M. Chou, et al., Expansion of rotational degrees of freedom for structural dynamic modification, *International Modal Analysis Conference V* 2 (1987) 950–955.
[14] E. Balmes, L. Billet, Using expansion and interface reduction to enhance structural modification methods, *International Modal Analysis Conference* XIX (2001) 615–621.
[15] S.W. Doebling, L.D. Peterson, K.F. Alvin, Estimation of reciprocal residual flexibility from experimental modal data, *AIAA Journal* 34 (8) (1996) 1678–1685.
[16] S.W. Doebling, L.D. Peterson, Computing statically complete flexibility from dynamically measured flexibility, *Journal of Sound and Vibration* 205 (5) (1997) 631–645.
[17] L.D. Peterson, K.F. Alvin, Determination of modal residues and residual flexibility for time-domain system realization, *ASME 15th Biennial Conference on Vibration and Noise*.
[18] N. Okubo, T. Matsuzaki, Determination of residual flexibility and its effective use in structural modification, *International Modal Analysis Conference* VII (1989) 578–583.
[19] R.C. Sohaney, D. Bonnecasse, Residual mobilities and structural dynamic modifications, *International Modal Analysis Conference* VII (1989) 568–574.
[20] P. Sjövall, T. Abrahamsson, Substructure system identification from coupled system test data, *Mechanical Systems and Signal Processing* 22 (2008) 15–33.
[21] W. D'Ambrogio, A. Fregolent, Decoupling of a substructure from modal data of the complete structure, *International Seminar on Modal Analysis* (2004) 2693–2706.
[22] E. Parloo, P. Verboven, P. Guillaume, M. Van Overmeire, Force identification by means of in-operational modal models, *International Modal Analysis Conference* (2002) 1159–1165.

[23] S. Vanlanduit, P. Guillaume, B. Cauberghe, E. Parloo, G. De Sitter, P. Verboven, On-line identification of operational loads using exogenous inputs, *Journal of Sound and Vibration* 285 (2005) 267–279.
[24] J.-S. Hwang, A. Kareem, W.-J. Kim, Estimation of modal loads using structural response, *Journal of Sound and Vibration* 326 (2009) 522–539.
[25] S. Li, Y. Liu, Parameter identification approach to vibration loads based on regularizing neural networks, *International Journal of Computer Science and Network Security* 6 (2006) 29–34.
[26] M. Djamaa, N. Ouelaa, C. Pezerat, J.L. Guyader, Reconstruction of a distributed force applied on a thin cylindrical shell by an inverse method and spatial filtering, *Journal of Sound and Vibration* 301 (2007) 560–575.
[27] J. O'Callahan, F. Piergentili, Force estimation using operational data, *International Modal Analysis Conference* XIV (1996) 1586–1592.
[28] E. Dascotte, J. Strobbe, Identification of a pressure forces in a cavity using an inverse solution method, *23rd International Seminar on Modal Analysis* (ISMA).
[29] H. Ahmadian, J.E. Mottershead, M.I. Friswell, Boundary condition identification by solving characteristic equations, *Journal of Sound and Vibration* 247 (5) (2001) 755–763.
[30] Y. Liu, W. Shepard Jr., Dynamic force identification based on enhanced least squares and total least-squares schemes in the frequency domain, *Journal of Sound and Vibration* 282 (2005) 37–60.
[31] M. Corus, E. Balmes, *A priori* verification of local fe model based force identification, *Proceedings of ISMA 2004 International Conference on Noise and Vibration Engineering*.
[32] B. Cauberghe, Applied Frequency-domain System Identification in the Field of Experimental and Operational Modal Analysis, PhD Thesis, Vrije Universiteit Brussel, 2004.
[33] B. Cauberghe, P. Guillaume, P. Verboven, E. Parloo, Identification of modal parameters including unmeasured forces and transient effects, *Journal of Sound and Vibration* 265 (2003) 609–625.
[34] S. Lu, Z.R. ans Law, Identification of system parameters and input force from output only, *Mechanical Systems and Signal Processing* 21 (2007) 2099–2111.
[35] M. Geradin, D. Rixen, *Mechanical Vibrations: Theory and Applications to Structural Dynamics*, second ed., Wiley, 1997.
[36] R.R. Craig, Coupling of substructures for dynamic analyses: an overview, AIAA Paper, No. 2000-1573, *AIAA Dynamics Specialists Conference*, 2000.
[37] R.R. Craig, M.C. Bampton, Coupling of substructures for dynamic analyses, *AIAA Journal* 6 (7) (1968) 1313–1319.
[38] R.H. MacNeal, A hybrid method of component mode synthesis, *Computers and Structures* 1 (1971) 581–601.
[39] G.M.L. Gladwell, Branch mode analysis of vibrating systems, *Journal of Sound and Vibration* 1 (1964) 41–59.
[40] S. Andrieux, Beam-3d, shell-3d coupling and generalization, Internal Report EDF-R&D Division.
[41] J. Bennighof, R. Lehoucq, An automated multilevel substructuring method for eigenspace computation in linear elastodynamics, *SIAM Journal on Scientific Computing* 25 (2003) 2004.
[42] J.M. Cros, Parallel modal synthesis methods in structural dynamics, *Contemporary Mathematics* 218 (1998) 492–499.
[43] R. Allemang, D. Brown, A correlation coefficient for modal vector analysis, *1st International Modal Analysis Conference* (IMAC), 1982, pp. 110–116.